The Journal of Immunology

Inhibition of B Cell Death Causes the Development of an IgA Nephropathy in (New Zealand White × C57BL/6)F_1-*bcl-2* Transgenic Mice

Regina Marquina, Miguel A. Díez, Marcos López-Hoyos, Luis Buelta, Aki Kuroki, Shuichi Kikuchi, Juan Villegas, Maria Pihlgren, Claire-Anne Siegrist, Manuel Arias, Shozo Izui, Jesús Merino and Ramón Merino

J Immunol 2004; 172:7177-7185; ;
doi: 10.4049/jimmunol.172.11.7177
http://www.jimmunol.org/content/172/11/7177

The Journal of Immunology is published twice each month by
The American Association of Immunologists, Inc.,
1451 Rockville Pike, Suite 650, Rockville, MD 20852

Print ISSN: 0022-1767 Online ISSN: 1550-6606.

Inhibition of B Cell Death Causes the Development of an IgA Nephropathy in (New Zealand White × C57BL/6)F_1-*bcl-2* Transgenic Mice[1]

Regina Marquina,[2]* Miguel A. Díez,[2]* Marcos López-Hoyos,[§] Luis Buelta,[†] Aki Kuroki,[‖] Shuichi Kikuchi,[‖] Juan Villegas,[‡] Maria Pihlgren,[‖] Claire-Anne Siegrist,[‖] Manuel Arias,[¶] Shozo Izui,[‖] Jesús Merino,[3,4]* and Ramón Merino[3,4]*

Little is known about the pathogenic mechanisms of IgA nephropathy, despite being the most prevalent form of glomerulonephritis in humans. We report in this study that in (New Zealand White (NZW) × C57BL/6)F_1 mice predisposed to autoimmune diseases, the expression of a human *bcl-2* (*hbcl-2*) transgene in B cells promotes a CD4-dependent lupus-like syndrome characterized by IgG and IgA hypergammaglobulinemia, autoantibody production, and the development of a fatal glomerulonephritis. Histopathological analysis of glomerular lesions reveals that the glomerulonephritis observed in these animals resembles that of human IgA nephropathy. The overexpression of Bcl-2 in B cells selectively enhances systemic IgA immune responses to T-dependent Ags. Significantly, serum IgA purified from (NZW × C57BL/6)F_1-*hbcl-2* transgenic mice, but not from nontransgenic littermates, shows reduced levels of galactosylation and sialylation and an increased ability to deposit in the glomeruli, as observed in human patients with IgA nephropathy. Our results indicate that defects in the regulation of B lymphocyte survival associated with aberrant IgA glycosylation may be critically involved in the pathogenesis of IgA nephropathy, and that (NZW × C57BL/6)F_1-*hbcl-2* Tg mice provide a new experimental model for this form of glomerulonephritis. ***The Journal of Immunology,*** **2004, 172: 7177–7185.**

Immunoglobulin A nephropathy (IgAN)[5] is the most common form of glomerulonephritis worldwide. Its clinical presentation may vary greatly from a primary nephropathy to a glomerulonephritis associated with several diseases, including autoimmune diseases such as systemic lupus erythematosus (SLE) or rheumatoid arthritis (1, 2). IgAN is unique among glomerular diseases in being defined by immunohistochemical findings rather than by light microscopy. The most common, but not exclusive, glomerular alteration associated with IgAN is the presence of focal or diffuse mesangial expansion of both extracellular matrix and cells (1, 2). The diagnosis of IgAN is based on the finding of IgA deposits in the mesangium that appear as an electron-dense material by electron microscopy (1–4). The presence of Ig deposits of IgG and IgM isotypes as well as C3 also can be observed in this type of nephropathy (3, 4).

Despite being so common, the etiology and the molecular and cellular mechanisms involved in IgAN remain largely unknown. It has been demonstrated recently that transgenic (Tg) mice overexpressing human FcαR on monocytes/macrophages develop an IgAN in association with the presence of circulating soluble FcαR-IgA complexes (5). Mesangial IgA deposition seems to be the final step resulting from different genetic and immunological abnormalities. Increased levels of circulating IgA1 and IgA plasma B cells, and altered mucosal (reduced) and systemic (enhanced) IgA immune responses are common immunological abnormalities observed in patients with IgAN (1, 2, 6–9). Multiple studies have reported that in these patients, IgA1 derived from sera and from diseased kidneys have a reduced pattern of galactosylation (10–13). Similar abnormalities are observed in HIGA (high IgA levels) mice bearing the ddY mutation, which spontaneously develop a glomerulonephritis resembling human IgAN (14, 15). Significantly, it has been shown that underglycosylated IgA1 has an increased capacity of self-aggregation and binding to human mesangial cells (12, 13), suggesting a nephritogenic potential of hypogalactosylated IgA.

Associations between defects in the regulation of lymphocyte apoptosis and autoimmune diseases have been reported repeatedly. The best example is the autoimmune lymphoproliferative syndrome observed both in humans and mice due to mutations in

*Laboratory of Immunology, Department of Molecular Biology, Unit Associated with Centro de Investigaciones Biologicas/Consejo Superior de Investigaciones Cientificas, and Departments of [†]Medical and Surgery Sciences and [‡]Anatomy and Cellular Biology, University of Cantabria, Santander, Spain; [§]Immunology and [¶]Nephrology, Hospital Universitario Marqués de Valdecilla, Santander, Spain; and [‖]Department of Pathology, University of Geneva, Geneva, Switzerland

Received for publication January 20, 2004. Accepted for publication March 22, 2004.

The costs of publication of this article were defrayed in part by the payment of page charges. This article must therefore be hereby marked *advertisement* in accordance with 18 U.S.C. Section 1734 solely to indicate this fact.

[1] This work was supported by Grant SAF00/0176 from the Ministerio de Ciencia y Tecnología (Spain) to J.M.; Grant SAF2002-02624 from the Ministerio de Ciencia y Tecnología (Spain) to R.M.; Grant FIS PI020417 from the Fondo de Investigación Sanitaria (Spain) to M.L.-H.; grants from the Fundación Marqués de Valdecilla (Spain) to J.M., R.M., M.A., and M.L.-H.; a grant from Swiss National Foundation to S.I.; and the "Instituto Reina Sofía de la Fundación Renal Iñigo Alvarez de Toledo" (Spain). R.M. is supported by the Ramón y Cajal Research Program, Ministerio de Ciencia y Tecnología (Spain).

[2] R.M. and M.A.D. contributed equally to this work.

[3] J.M. and R.M. share senior authorship.

[4] Address correspondence and reprint requests to Drs. Ramón Merino and Jesús Merino, Laboratorio de Inmunología, Departamento de Biología Molecular, Facultad de Medicina, Universidad de Cantabria, Cardenal Herrera Oria s/n, 39011 Santander, Spain. E-mail address: merinor@unican.es

[5] Abbreviations used in this paper: IgAN, IgA nephropathy; ASC, Ab-secreting B cell; *hbcl-2*, human *bcl-2*; HEL, hen egg lysozyme; HIGA, high Ig level; IC, immune complex; MZ, marginal zone; NZW, New Zealand White; PP, Peyer's patch; RCA-I, *Ricinus communis* agglutinin I; RF, rheumatoid factor; SLE, systemic lupus erythematosus; SNA, elderberry (*Sambucus nigra*) bark lectin; Tg, transgenic; TNP, 2,4,6-trinitrophenyl; TT, tetanus toxoid; TU, titration unit.

0022-1767/04/$02.00

fas/fasL or different caspases (16, 17). Mice with a targeted disruption of *bim*, a proapoptotic *bcl-2* relative, develop an autoimmune syndrome resembling SLE (18). The absence of *bim* results in alterations in the elimination of autoreactive T cells within the thymus and in the control of cell death of Ag-activated T cells during termination of an immune response (19, 20). However, in other situations in which the inhibition of cell death induces the development of autoimmune diseases, such as is observed in Tg mice overexpressing Bcl-2 in B cells, the mechanisms involved in the pathogenesis of the disease are less clear (21). In an attempt to explore in more detail the relationship between the inhibition of B cell apoptosis and the development of systemic autoimmune diseases, we have generated (New Zealand White (NZW) × C57BL/6)F_1 mice overexpressing a human *bcl-2* (*hbcl-2*) transgene in B cells. These Tg mice spontaneously develop a CD4-dependent autoimmune syndrome, which is characterized by IgG and IgA hypergammaglobulinemia, the production of several autoantibodies, and the development of a lethal glomerulonephritis. Unexpectedly, histopathological analysis reveals that the glomerular disease observed in these animals resembles human IgAN, and is associated with a reduced sialylation and galactosylation of circulating IgA. We propose (NZW × B6)F_1-*hbcl-2* Tg mice as a new experimental model to explore in vivo cellular and molecular mechanisms involved in IgAN.

Materials and Methods

Mice, treatments, and immunizations

B6, B6-SV40-Eμ-*hbcl-2*-22 Tg (B6-*hbcl-2* Tg) (21), and NZW mice were purchased from The Jackson Laboratory (Bar Harbor, ME). B6 μMT mice (22) were kindly provided by K. Rajewsky (Cologne, Germany). The F_1 hybrids used in this study were obtained in our animal facilities. The presence of the *hbcl-2* Tg in F_1 mice was assessed in PBMC by flow cytometry using a specific mAb against human Bcl-2 (clone 6C8; BD PharMingen, San Diego, CA), as described previously (23). In *B6-hbcl-2* Tg mice, the expression of the *hbcl-2* transgene is controlled by the SV40 promoter and Eμ enhancer and promotes the overexpression of hBcl-2 in all subpopulations of developing and peripheral mature B cells, but not in T or dendritic cells (21) (data not shown). Mice were bled every 2 mo from the retro-orbital plexus, and the resulting sera were stored at −20°C until use.

To evaluate the role of $CD4^+$ T cells in the development of autoimmune disease, (NZW × B6)F_1-*hbcl-2* Tg mice were treated from birth until 6 mo with an anti-CD4 mAb (GK-1.5: rat IgG2b), as described previously (24). The efficiency of this treatment was evaluated monthly in PBMC by flow cytometry.

To explore the effects of hBcl-2 overexpression in B cells in the development of IgG and IgA T-dependent immune responses, 8-wk-old B6-*hbcl-2* Tg and non-Tg mice were immunized i.p. with 100 μg of hen egg lysozyme (HEL) emulsified in CFA. Primary IgG and IgA anti-HEL immune responses were evaluated 2 and 4 wk after immunization by ELISA. Mice were challenged i.p. with 100 μg of HEL dissolved in PBS 1 and 2 mo after primary immunization, and IgG and IgA secondary and tertiary anti-HEL Ab responses were evaluated 2 and 4 wk later. In addition, 8-wk-old B6-*hbcl-2* Tg and non-Tg mice were immunized i.p. with 50 μg of 2,4,6-trinitrophenyl $(TNP)_{11}$-OVA (Biosearch Technologies, Novato, CA) mixed with $Al(OH)_3$ and boosted with the same dose of Ag 4 and 8 wk later. The titers of high affinity IgG and IgA anti-TNP_3 Abs were evaluated 2 and 4 wk after each immunization, by ELISA on polystyrene microtiter plates (Flow Laboratories, McLean, VA) coated with 10 μg/ml BSA-TNP_3 (Biosearch Technologies). Results of anti-HEL and anti-TNP_3 Abs were expressed in titration units (TU) in reference to serum pools from immunized adult mice. To determine the number of anti-tetanous toxoid (TT) Ab-secreting B cells (ASC), 8-wk-old B6-*hbcl-2* Tg and non-Tg mice were immunized i.p. with 3 μg of TT (Anatoxal TE, Berna, Switzerland) in a volume of 100 μl of saline solution containing 500 μg of $Al(OH)_3$. Animals were boosted with the same dose of Ag 15 days later. All in vivo experiments with mice were performed in compliance with the Guide for the Care and Use of Laboratory Animals (25).

Enumeration of anti-TT ASC by ELISPOT

The TT-specific ASC number was assessed by ELISPOT, as previously described (26). Briefly, single-cell suspensions were obtained from the spleen of B6-*hbcl-2* Tg and non-Tg mice 21 days after secondary immunization with TT-$Al(OH)_3$ and resuspended in complete DMEM (Life Technologies, Gaithersburg, MD) containing 10% FCS. The spleen cell suspensions were then treated with ammonium citrate potassium lysing buffer (0.15 M NH_4CL, 10 mM $KHCO_3$, and 0.1 mM Na_2EDTA) to eliminate RBC. Multiscreen HA nitrocellulose-bottom plates (Millipore, Bedford, MA) were coated with 10 μg/ml TT overnight at 37°C. After washing with PBS-0.1% Tween 20 and blocking with DMEM containing 10% FCS, serial dilutions of the single-cell suspension were added to the plates and incubated for 5 h at 37°C. After washing, plates were incubated with alkaline phosphatase-conjugated goat anti-mouse IgG or IgA (Serotec, Oxford, U.K., and ICN Biomedicals, Irvine, CA, respectively) overnight at 4°C, washed, and incubated with 5-bromo-4-chloro-3-indolyl phosphate/nitroblue tetrazolium substrate (Sigma-Aldrich, Madrid, Spain). Wells containing between 10 and 70 spots (linear zone) were counted by eye. In addition, total IgA ASC in spleen and Peyer's patches (PP) from nonimmunized 4-mo-old (NZW × B6)F_1-*hbcl-2* Tg and non-Tg mice were also evaluated by ELISPOT using Multiscreen HA nitrocellulose-bottom plates coated with 10 μg/ml goat anti-IgA Abs, as described above.

Flow cytometry studies

The number of marginal zone (MZ) B cells in the spleen, B-1a cells in the peritoneal cavity, and $B220^+CD138^+$ plasma B cells in the spleen and PP in (NZW × B6)F_1 non-Tg and (NZW × B6)F_1-*hbcl-2* Tg mice was evaluated by flow cytometry. Single-cell suspensions from spleen and peritoneal cells, obtained after washing the peritoneal cavity with 10 ml of ice-cold PBS containing 5% of FCS, were stained with different combinations of FITC-, PE-, PerCP-, and biotin-conjugated mAbs (BD PharMingen) directed against surface B cell Ags. The following anti-mouse mAbs were used: FITC-conjugated anti-CD21 (clone 7G6), PE-conjugated anti-CD138 (clone 281-2), PE-conjugated anti-CD5 (clone 53-7.3), PE-conjugated anti-CD23 (clone B3B4), PerCP-conjugated anti-B220 (clone RA3-6B2), and biotin-conjugated anti-IgM (clone R6-60.2). For biotinylated mAbs, PE-conjugated streptavidin (BD PharMingen) was used as a second step reagent. A total of 5×10^4 viable cells was analyzed in a FACSCalibur flow cytometer using CellQuest Pro software (BD Biosciences, Mountain View, CA).

Serological studies

Serum levels of total IgG1, IgG2a, IgG2b, IgG3, and IgA were determined by ELISA. Briefly, plates were coated with rabbit anti-mouse IgG subclass-specific (Serotec) or goat anti-mouse IgA-specific Abs, and the assays were developed with the same corresponding Abs conjugated to alkaline phosphatase. None of the subclass- or isotype-specific Abs used in this study were cross-reactive with other Ig isotypes (data not shown). Results were expressed in mg/ml in reference to a standard curve obtained with a mouse reference serum (ICN Biomedicals). The presence of IgG and IgA anti-DNA autoantibodies was determined in sera by ELISA. ssDNA from calf thymus (Sigma-Aldrich) was used at a concentration of 10 μg/ml for coating the wells of polystyrene microtiter plates (Flow Laboratories). After incubation with 1/100 diluted serum samples, bound IgA and IgG were detected with alkaline phosphatase-conjugated goat anti-IgA or anti-IgG Abs, respectively. Results were expressed in TU in reference to a standard curve obtained from a serum pool from 6- to 8-mo-old MRL *lpr/lpr* mice. Serum levels of gp70 immune complexes (IC) were quantified by ELISA (24), and the results were expressed as μg of Ab-bound gp70/ml serum. Serum levels of IgM anti-Bromelain-treated mouse RBC autoantibodies were measured, as described previously (27).

Serum pools from 4- to 6-mo-old (NZW × B6)F_1 non-Tg and (NZW × B6)F_1-*hbcl-2* Tg mice were prepared by mixing 50 μl of 10–15 sera in each different pool. IgA, IgG, and IgM were purified from each pool using KATIV-AE affinity column (Genomics One International, Buffalo, NY), protein G affinity column (Amersham Pharmacia Biotech, Barcelona, Spain), and LOMM-9 affinity column chromatography, respectively. The purity of IgA, IgG, or IgG samples thus obtained was confirmed by isotype-specific ELISA. The pattern of galactosylation and sialylation of IgA, IgG, and IgM was assessed by a lectin-binding assay combined with ELISA, using biotinylated elderberry (*Sambucus nigra*) bark lectin to detect sialic acid (SNA; Vector Laboratories, Burlingame, CA) and *Ricinus communis* agglutinin I (RCA-I; Vector Laboratories) to detect galactose residues (28). Different concentrations of purified IgA, IgG, or IgM diluted in PBS were used for coating the wells of polystyrene microtiter plates (Linbro Titertek; ICN Biomedicals). After washing, wells were incubated first with biotinylated lectins at 10 μg/ml and then with alkaline phosphatase-conjugated streptavidin (BD PharMingen). Glycosylation was expressed as percentage of binding calculated by the following formula: (OD

developed with the lectin detection system/OD developed with anti-IgA, anti-IgG, or anti-IgM alkaline phosphatase conjugates) × 100.

IgA clearance and glomerular deposition studies

To explore possible differences in the clearance of IgA from (NZW × B6)F_1-*hbcl-2* Tg and non-Tg mice, separate groups of Ig-deficient B6 μMT mice were injected i.v. with 0.2 ml (1 mg) of purified IgA of each mouse strain. Mice were bled at serial time points after the injection. Serum concentrations of IgA were determined by ELISA. The amount of IgA remaining in blood was calculated relative to the value 5 min after the injection.

To analyze whether hypoglycosylated IgA from (NZW × B6)F_1-*hbcl-2* Tg mice has an increased glomerular deposition capacity than IgA from (NZW × B6)F_1 non-Tg mice, groups of 1.5-mo-old (NZW × B6)F_1 non-Tg mice (3 mice/group) received a daily i.v. injection during 3 consecutive days of 3.3 mg of purified IgA from each 8-mo-old F_1 mice (total amount: 10 mg/mice), separately. The presence of IgA deposits in the glomeruli of Ig-injected (NZW × B6)F_1 non-Tg mice was explored by immunofluorescence 24 h after the last injection, as described below.

Quantitative real-time RT-PCR analyses

Spleens from (NZW × B6)F_1-*hbcl-2* Tg and non-Tg mice were homogenized with a Polytron (IKA Labortechnik, Staufen, Germany), and total RNA was isolated using the Ultraspec RNA reagent (Biotecx, Houston, TX). For RT-PCR, 2 μg of DNase I-treated RNA was reverse transcribed with murine leukemia virus reverse transcriptase (Roche Diagnostics, Lewes, U.K.). To measure the expression of TGF-β1 in the spleen of these mouse strains, real-time PCR was performed in an ABI-Prism 700 cycler system (Applied Biosystems, Foster City, CA) using primers from different exons that generated a product of ~200 bp in length. Results (in triplicates) are normalized to GAPDH expression and measured in parallel in each sample.

Proteinuria and histopathology

Proteinuria was assessed by determination of urine albumin using reagent striped Albustix (Bayer, Barcelona, Spain) and scored in a 0–4 scale in which 0 indicates the absence or traces of proteinuria, 1 indicates proteinuria values between 30 and 100 mg/dl, 2 indicates proteinuria values between 100 and 300 mg/dl, 3 indicates proteinuria values between 300 and 1000 mg/dl, and 4 indicates proteinuria values higher than 1000 mg/dl. Proteinuria of 2 or more was considered as positive.

Samples of all major organs were obtained at autopsy. Most organs were included in paraffin and stained with H&E for pathological studies. For kidney light and electron microscopy studies, the organs were immersed in a fixative solution containing 3% glutaraldehyde in 0.12 M PBS (pH 7.4) for 24 h at room temperature. After fixation, 300-μm-thick sections were obtained in a vibratome, and small blocks from the cortex were dissected out and postfixed in 2% osmium tetroxide (in 0.12 M PBS), dehydrated, and embedded in Durcupan (Fluka, Buchs, Switzerland; Sigma-Aldrich). For light microscopy examination, semithin sections (1 μm) were stained with 1% toluidine blue. Glomerulonephritis was scored on a 0–4 scale, as described previously (29). In addition, ultrathin sections were cut on a LKB ultramicrotome (LKB Instruments, Gaithersburg, MD), counterstained with 3% uranyl acetate, followed by lead citrate, and examined in a Philips EM-208 electron microscope. All histological preparations were analyzed in a blinded fashion by a pathologist.

Tissue-bound IgM, IgG, and IgA Abs were studied by immunofluorescence on kidney cryosections using FITC-conjugated goat anti-mouse IgM and IgG Abs (Jackson ImmunoResearch Laboratories, West Grove, PA) or FITC-conjugated goat anti-mouse IgA Ab (Cappel Laboratories, Cochranville, PA).

Statistical analysis

Statistical analysis of differences between groups of mice was performed using the Mann-Whitney *U* test. Probability values <0.05 were considered significant.

Results

*Development of an IgAN associated with a lupus-like autoimmune syndrome in (NZW × B6)F_1-*hbcl-2 *Tg mice*

To study how alterations in the regulation of B cell apoptosis may result in autoimmune diseases, B6-*hbcl-2* Tg mice (21) were crossed with NZW mice. (NZW × B6)F_1-*hbcl-2* Tg mice developed a severe autoimmune syndrome. At 4 mo of age, these Tg mice spontaneously produced increased levels of serum IgG1, IgG2a, IgG2b, IgG3, and IgA Abs in comparison with (NZW × B6)F_1 non-Tg controls (Fig. 1; $p < 0.01$ in all cases). These mice also had higher titers of IgG and IgA anti-DNA autoantibodies and of gp70 IC in their sera than non-Tg F_1 mice (Fig. 2; $p < 0.001$ in all cases). The enhanced IgA autoantibody production in (NZW × B6)F_1-*hbcl-2* Tg mice was accompanied by a parallel increase in the number of splenic total IgA and $B220^+CD138^+$ plasma cells. Thus, 4-mo-old (NZW × B6)F_1-*hbcl-2* Tg mice exhibited a 19- and 25-fold increase in the number of splenic total IgA ASC ($1.5 \times 10^6 \pm 0.4 \times 10^6$ cells; $n = 5$) and $B220^+CD138^+$ plasma cells ($36.3 \times 10^6 \pm 12.4 \times 10^6$ cells; $n = 5$), respectively, in comparison with (NZW × B6)F_1 non-Tg mice (total IgA ASC, $0.8 \times 10^5 \pm 0.1 \times 10^5$ cells; $B220^+CD138^+$ plasma cells, $1.5 \times 10^6 \pm 0.3 \times 10^6$ cells; $n = 4$). This increment was also observed, although at a much lower extent, in the PP of (NZW × B6)F_1-*hbcl-2* Tg mice (number of total IgA ASC in PP of (NZW × B6)F_1-*hbcl-2* Tg mice, $1.4 \times 10^4 \pm 0.2 \times 10^4$ cells; in (NZW × B6)F_1 non-Tg mice, $0.4 \times 10^4 \pm 0.03 \times 10^4$ cells (3.5-fold increase); number of $B220^+CD138^+$ plasma cells in PP of (NZW × B6)F_1-*hbcl-2* Tg mice, $1.7 \times 10^4 \pm 0.6 \times 10^4$ cells; in (NZW × B6)F_1 non-Tg mice, $0.6 \times 10^4 \pm 0.08 \times 10^4$ cells (3-fold increase)). Interestingly, we had recently reported that (NZW × B6)F_1-*hbcl-2* Tg, but not non-Tg mice produced increased levels of IgG rheumatoid factor (RF) autoantibodies (30). The increased anti-IgG RF autoantibody production observed in (NZW × B6)F_1-*hbcl-2* Tg mice might account for the elevated titers of IgA anti-

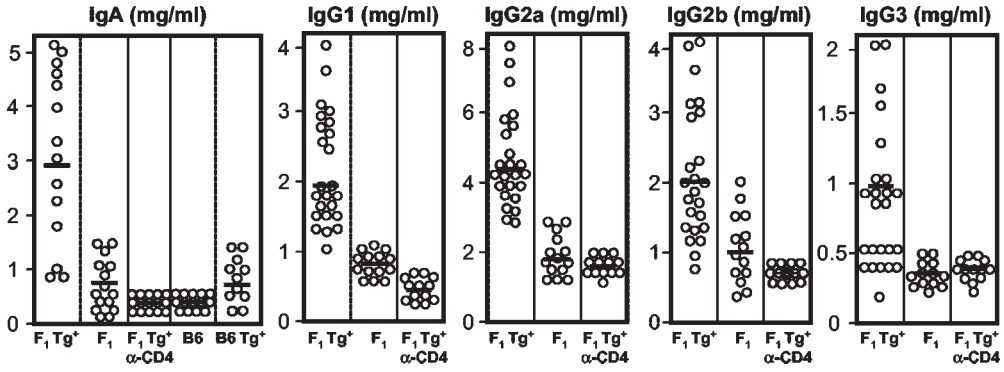

FIGURE 1. Serum levels of IgA and IgG subclasses in 4-mo-old (NZW × B6)F_1 non-Tg, (NZW × B6)F_1-*hbcl-2* Tg, and anti-CD4-treated (NZW × B6)F_1-*hbcl-2* Tg mice, and serum levels of IgA in 4-mo-old B6 non-Tg and B6-*hbcl-2* Tg mice. Values of individual mice are expressed in mg/ml. Bars represent the mean value of each examination.

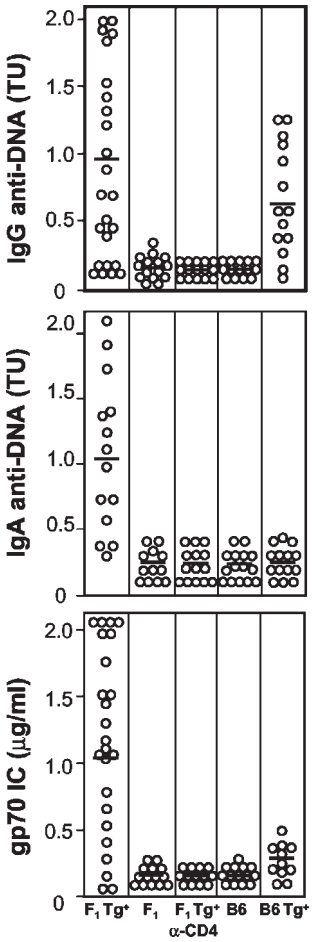

FIGURE 2. Serum levels of IgG and IgA anti-DNA and of gp70 IC in 4-mo-old (NZW × B6)F_1 non-Tg, (NZW × B6)F_1-*hbcl-2* Tg, anti-CD4-treated (NZW × B6)F_1-*hbcl-2* Tg, B6 non-Tg, and B6-*hbcl-2* Tg mice. Values of individual mice are expressed in TU for anti-DNA autoantibodies and in μg/ml for gp70 IC. Bars represent the mean value of each examination.

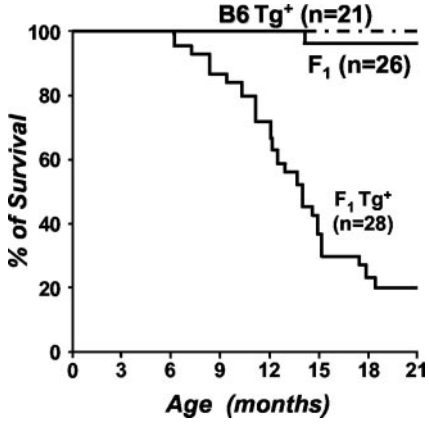

FIGURE 3. Mortality curve of (NZW × B6)F_1 non-Tg, (NZW × B6)F_1-*hbcl-2* Tg, and B6-*hbcl-2* Tg mice.

DNA autoantibody production observed in these animals. However, although the production of IgA anti-IgG RF autoantibodies was not explored in our previous study, the increased numbers of total IgA ASC and IgA Ag-specific ASC (see below) observed in *hbcl-2* Tg mice strongly argue against such possibility. In correlation with these serological parameters, (NZW × B6)F_1-*hbcl-2* Tg mice showed a shortened life span, with a 50% cumulative mortality rate at 13 mo of age and 80% at 18 mo of age (Fig. 3). Notably, none of the non-Tg F_1 littermates died by 18 mo of age. The accelerated mortality of (NZW × B6)F_1-*hbcl-2* Tg mice was preceded by the presence of intense proteinuria (mean score of proteinuria at 9 mo of age: 3.3 ± 0.9; $n = 14$) that was not observed in (NZW × B6)F_1 non-Tg controls (mean score of proteinuria at 9 mo of age: 1.1 ± 1.4; $n = 11$).

Histological analysis of major organs at 8–12 mo of age indicated that the majority of (NZW × B6)F_1-*hbcl-2* Tg mice, but none of the non-Tg littermates, developed a severe and diffuse glomerulonephritis (mean histological grades of glomerular lesions in Tg mice, 3.75 ± 0.62, $n = 12$; in non-Tg mice, 0.67 ± 1.03, $n = 6$, $p < 0.001$), characterized by intense mesangial hypercellularity in association with immune deposits (Fig. 4, *A* and *B*). In addition, in 37.6% of Tg mice, but not in non-Tg controls, clear signs of tubular atrophy and interstitial fibrosis were also observed (Fig. 4, *C* and *D*). The presence of proteinuria together with the histopathological kidney lesions observed in (NZW × B6)F_1-*hbcl-2* Tg mice suggest that this severe form of glomerulonephritis was likely to be the principal cause for the accelerated mortality. In fact, other histopathological lesions, such us lymphoproliferative disorders, were not observed in these animals. Ultrastructural inspection of affected glomeruli from (NZW × B6)F_1-*hbcl-2* Tg mice revealed basement membrane thickening in glomerular capillaries and the presence of electron-dense deposits in both subepithelial (Fig. 5*C*) and mesangial regions (Fig. 5*D*). In association with these electron-dense deposits, there was an intense hypercellularity in the mesangium of affected glomeruli (Fig. 5*B*). In contrast, glomeruli from (NZW × B6)F_1 non-Tg mice showed a normal appearance, and electron-dense deposits were hardly observed within glomeruli (Fig. 5*A*).

Immunofluorescence studies showed the presence of mesangial IgM deposits with a granular distribution in (NZW × B6)F_1-*hbcl-2* Tg mice at an extent much greater than that observed in (NZW × B6)F_1 non-Tg and NZW mice (Fig. 4*H* and Table I). Despite the high levels of circulating total IgG and IgG autoantibodies, (NZW × B6)F_1-*hbcl-2* Tg mice presented little, if any, IgG deposits in their glomeruli in comparison with aged-matched lupus-prone (New Zealand Black × NZW)F_1 female mice used as positive controls (Fig. 4, *J* and *K*; Table I). However, prominent granular IgA deposits localized primarily in the mesangium were observed in (NZW × B6)F_1-*hbcl-2* Tg mice, but not in (NZW × B6)F_1 non-Tg and NZW mice (Fig. 4*I* and Table I). Thus, the combination of light and electron microscopy findings, together with the immunofluorescence studies, indicated that the glomerulonephritis observed in (NZW × B6)F_1-*hbcl-2* Tg mice resembles an IgAN.

Because multiple genetic factors are involved in the pathogenesis of both IgAN and SLE (31, 32) and because NZW mice have several dominant genetic loci linked with lupus traits (32–34), the importance of the genetic background in the development of autoimmune syndrome in (NZW × B6)F_1-*hbcl-2* Tg mice was explored using B6-*hbcl-2* Tg mice. In contrast to (NZW × B6)F_1-*hbcl-2* Tg mice, B6-*hbcl-2* Tg mice failed to produce IgA anti-DNA autoantibodies and gp70 IC ($p > 0.5$ and $p > 0.2$, respectively), despite a significant production of IgG anti-DNA autoantibodies (Fig. 2, $p < 0.005$). Serum levels of IgA in B6-*hbcl-2* Tg mice were hardly elevated, and not higher than those in (NZW × B6)F_1 non-Tg mice (Fig. 1, $p > 0.5$). Notably, B6-*hbcl-2* Tg mice showed a normal life span (Fig. 3) with no sign of glomerulonephritis (Fig. 4, *F* and *G*; Table I).

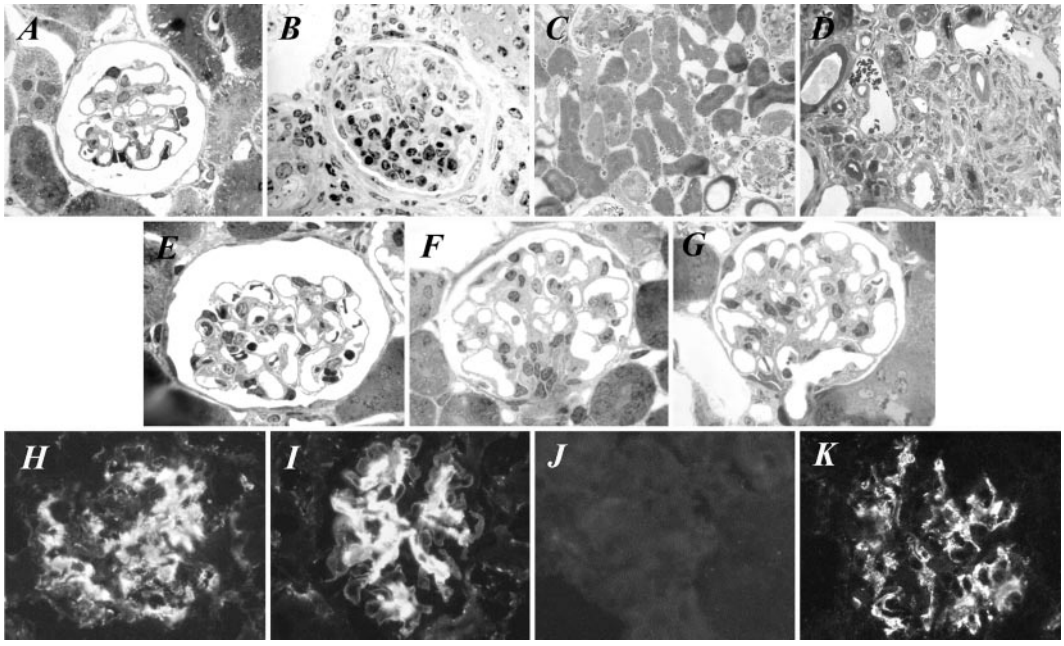

FIGURE 4. Representative histological appearance of glomeruli (×40) from 8-mo-old (NZW × B6)F_1 non-Tg mice (*A*) and (NZW × B6)F_1-*hbcl-2* Tg mice (*B*), tubules (×10) from 8-mo-old (NZW × B6)F_1 non-Tg mice (*C*) and (NZW × B6)F_1-*hbcl-2* Tg mice (*D*), glomeruli (×40) from 6-mo-old anti-CD4-treated (NZW × B6)F_1-*hbcl-2* Tg mice (*E*) and 8-mo-old B6 non-Tg mice (*F*), and B6-*hbcl-2* Tg mice (*G*). Presence of IgM (*H*), IgA (*I*), and IgG (*J*) deposits in the glomeruli of 6-mo-old (NZW × B6)F_1-*hbcl-2* Tg mice and IgG glomerular deposits (*K*) in 6-mo-old (New Zealand Black × NZW)F_1 female mice (×40).

The development of both IgAN and SLE in (NZW × B6)F_1-hbcl-2 Tg mice is dependent on CD4$^+$ T cells.

To assess the role of CD4$^+$ T cells in the development of IgAN and SLE in (NZW × B6)F_1-*hbcl-2* Tg mice, Tg F_1 animals were treated from birth with an anti-CD4 mAb. This treatment induced a complete and persistent depletion of CD4$^+$ T cells, documented by flow cytometric analysis (data not shown). The depletion of CD4$^+$ T cells in (NZW × B6)F_1-*hbcl-2* Tg mice was followed by the complete inhibition of autoimmune manifestations. The levels of circulating IgG subclasses and IgA (Fig. 1), IgG, and IgA anti-DNA autoantibodies and gp70 IC (Fig. 2) in 4-mo-old CD4$^+$-depleted (NZW × B6)F_1-*hbcl-2* Tg mice were similar or even lower than those found in untreated (NZW × B6)F_1 non-Tg controls. When evaluated for renal histopathology at 6 mo of age, CD4$^+$-depleted (NZW × B6)F_1-*hbcl-2* Tg mice showed minimal glomerular alterations (Fig. 4*E*), in clear contrast with the significant glomerular lesions observed in untreated Tg mice (Fig. 4*B*).

Overexpression of Bcl-2 in B cells enhances systemic IgA immune responses to T-dependent Ags

It has been shown that patients with IgAN mount abnormal mucosal and systemic IgA immune responses to T-dependent Ags (8, 9). To analyze whether the overexpression of Bcl-2 in B cells influenced systemic IgA Ab responses, serum levels of IgA and IgG Abs during primary, secondary, and tertiary immune responses against T-dependent Ags were compared between B6-*hbcl-2* Tg and non-Tg mice. Both B6-*hbcl-2* Tg and non-Tg mice developed high affinity IgG anti-TNP_3 Ab responses after immunization with TNP_{11}-OVA. The levels of high-affinity IgG anti-TNP_3 Abs in B6-*hbcl-2* Tg mice were slightly higher ($p < 0.01$) than in non-Tg littermates after primary immunization, but no longer different after secondary or tertiary immunization (Fig. 6*A*). However, primary, secondary, and tertiary high-affinity IgA anti-TNP_3 Ab responses were observed only in B6-*hbcl-2* Tg mice (Fig. 6*B*; $p < 0.001$ in all cases). These results were confirmed using another T-dependent Ag, HEL. B6-*hbcl-2* Tg mice developed higher primary, but comparable secondary and tertiary IgG anti-HEL Ab responses after immunization with HEL (Fig. 6*C*). Again, IgA anti-HEL Ab levels were very significantly enhanced after each immunization in mice overexpressing Bcl-2 in B cells (Fig. 6*D*). Enhanced IgA immune responses to T-dependent Ags in *hbcl-2* Tg mice were further confirmed by enumeration of IgG and IgA anti-TT ASC, as measured by ELISPOT, in the spleen 21 days after secondary immunization with TT-$Al(OH)_3$. In fact, B6-*hbcl-2* Tg and non-Tg mice showed comparable numbers of IgG anti-TT ASC per spleen after secondary immunization with TT, while the overexpression of hBcl-2 in B cells promoted a remarkable expansion of IgA ASC per spleen (15 times), in comparison with that observed in B6 non-Tg controls (Table II; $p < 0.001$).

The marked increase of Ag-specific IgA ASC in *hbcl-2* Tg mice can be a result of an expansion of B-1 cells, as proposed in humans (35), or MZ B cells, which share many phenotypic characteristics of B-1 cells (36). However, the total number of B-1 cells in the peritoneal cavity of both strains of mice was essentially identical (means of 5 mice ± SD: 3-mo-old (NZW × B6)F_1-*hbcl-2* Tg mice, 4.4 ± 1.3 × 10^6; and in 3-mo-old (NZW × B6)F_1 non-Tg mice, 6.5 ± 1.8 × 10^6). This was consistent with the finding that the serum levels of IgM anti-Bromelain-treated mouse RBC, selectively produced by B-1 cells (35), were comparable between (NZW × B6)F_1-*hbcl-2* Tg and non-Tg mice (data not shown). In contrast, the overexpression of hBcl-2 in B cells from (NZW × B6)F_1-*hbcl-2* Tg mice resulted in a reduction in the size of MZ B cell compartment (means of 5 mice ± SD: percentage of B220$^+$-CD21^{high}-CD23$^{negative/low}$ MZ B cells in spleen cells from 3-mo-old (NZW × B6)F_1-*hbcl-2* Tg mice, 0.7 ± 0.2%; and from 3-mo-old (NZW × B6)F_1 non-Tg mice, 7.4 ± 2.5%), as reported recently in B6-*hbcl-2* Tg mice (37). We also determined whether (NZW × B6)F_1-*hbcl-2* Tg mice exhibited an increased expression of TGF-β, a cytokine involved in the induction and differentiation of

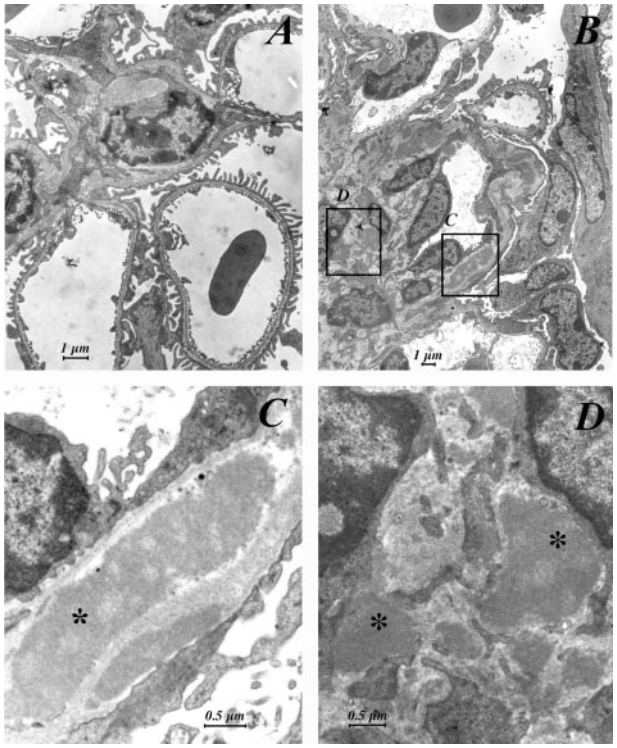

FIGURE 5. *A*, Electron micrograph of glomerular capillaries from 8-mo-old (NZW × B6)F_1 non-Tg mice showing endothelial cells, basement membrane, epithelial cells, and mesangial cells with a normal appearance. *B*, Ultrastructural analysis of affected glomeruli in kidneys from (NZW × B6)F_1-*hbcl-2* Tg mice shows mesangial hypercellularity, basement membrane thickening in glomerular capillaries, and electron-dense deposits in both subepithelial and mesangial regions. *C* and *D*, Detailed view of the squared regions in *B* showing subepithelial (*C*) and mesangial (*D*) deposits (asterisks). Three mice were analyzed in each group.

IgA-secreting plasma cells (38, 39), in their secondary lymphoid organs. However, quantitative real-time RT-PCR analysis failed to show any significant differences in the levels of TGF-β1 mRNA in the spleen between 6-mo-old (NZW × B6)F_1-*hbcl-2* Tg (TGF-β1/GAPDH ratio: 0.841 ± 0.014, $n = 5$) and non-Tg mice (0.987 ± 0.006, $n = 4$).

Abnormal glycosylation of serum IgA in mice overexpressing hBcl-2 in B cells

The development of IgAN both in humans and in HIGA mice has been associated with a reduced galactosylation of IgA (10–13, 15). To explore whether similar changes in IgA galactosylation were observed in (NZW × B6)F_1-*hbcl-2* Tg mice in association with the development of IgAN, circulating IgA was purified from serum pools from 4- to 6-mo-old (NZW × B6)F_1-*hbcl-2* Tg and non-Tg F_1 mice. Murine IgA bear a series of bi-antennary and tri-antennary complex-type oligosaccharide chains, and the terminal residues are heterogeneous, either ending by sialic acid, galactose, or *N*-acetylglucosamine, in which the terminal sialylation is dependent on the galactosylation, because sialic acids are linked to galactose residues (40). Thus, the extent of galactosylation and sialylation was assessed by determining the interaction of IgA with two different lectins, SNA and RCA-I, which specifically recognize sialic acid and galactose, respectively (28). SNA and RCA-I lectin-binding assays revealed that galactosylation and sialylation levels of IgA from five different serum pools of (NZW × B6)F_1-*hbcl-2* Tg mice were reduced by ~50% in comparison with that

Table I. *Increased deposits of IgA, but not of IgG, in the glomeruli of (NZW × B6) F_1-hbcl-2 Tg mice*[a]

Mice	IgM	IgG	IgA
B6 non-Tg	−	−	−
B6-*hbcl-2* Tg	−	−	−
NZW	++	−	−
(NZB × NZW)F_1	+++	+++	ND
(NZW × B6)F_1 non-Tg	++	−	−
(NZW × B6)F_1-*hbcl-2* Tg	+++	−	+++

[a] The presence of glomerular IgM, IgG, and IgA deposits in the different strain of mice ($n = 3$ mice/group) was evaluated by immunofluorescence on kidney cryosections at 6 mo of age. The intensity of fluorescence is indicated (0 to +++). ND, not done.

observed in IgA from five independent non-Tg F_1 serum pools (Fig. 7*A*; $p < 0.005$).

To verify whether the abnormal Ig glycosylation pattern observed in (NZW × B6)F_1-*hbcl-2* Tg mice was specific to IgA, serum IgG and IgM purified from (NZW × B6)F_1-*hbcl-2* Tg and non-Tg F_1 mice were similarly subjected to the lectin-binding assays. In contrast to IgA, IgG and IgM from three independent serum pools of 4- to 6-mo-old (NZW × B6)F_1-*hbcl-2* Tg and non-Tg mice exhibited comparable bindings to both SNA and RCA-I lectins (Fig. 7, *B* and *C*; $p > 0.5$ in both cases), indicating no measurable alterations in the galactosylation and sialylation of oligosaccharide chains attached to IgG or IgM from (NZW × B6)F_1-*hbcl-2* Tg mice.

In human patients with IgAN, it has been demonstrated that hypoglycosylated IgA1 apparently has an increased capacity of binding to glomerular mesangial cells (12, 13). It also has been claimed that hypoglycosylated IgA1 from patients with IgAN has a longer $t_{1/2}$ than IgA1 from healthy donors when injected into

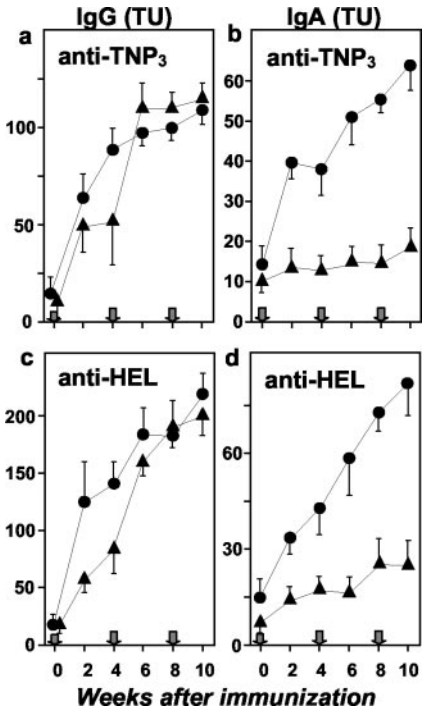

FIGURE 6. Serum levels of IgG (*A*) and IgA (*B*) anti-TNP_3 Abs and of IgG (*C*) and IgA (*D*) anti-HEL Abs after primary, secondary, and tertiary immunization in B6 non-Tg mice (▲) and B6-*hbcl-2* Tg mice (●). Mean levels (±1 SD) are expressed in TU in reference to serum pools from immunized adult mice (7–10 mice in each group). Arrows indicate the time of each immunization.

Table II. *Expansion of IgA, but not IgG anti-TT ASC in B6-hbcl-2 Tg mice*[a]

Mice	Immunization	IgG anti-TT ASC	IgA anti-TT ASC
Non-Tg	PBS	41.4 ± 7.9	14.3 ± 3.8
Non-Tg	TT-$Al(OH)_3$	3970.8 ± 207.1	67.2 ± 10.1
bcl-2-Tg	PBS	60.8 ± 16.1	30.4 ± 12.4
bcl-2-Tg	TT-$Al(OH)_3$	4561.4 ± 335.6	1033.7 ± 298.6

[a] Eight-week-old B6-*hbcl-2* Tg and non-Tg mice were immunized l.p. with 3 μg of TT-$Al(OH)_3$. Animals were boosted with the same dose of Ag 15 days later. ASC were measured by ELISPOT in the spleen 21 days after secondary immunization. Results are expressed as the mean number of ASC ± SD in the total spleen (4 animals/group).

mice (13, 41). To explore whether hypoglycosylated IgA from (NZW × B6)F_1-*hbcl-2* Tg mice exhibited similar characteristics, the serum clearance and glomerular deposition of IgA from (NZW × B6)F_1-*hbcl-2* Tg and non-Tg mice were compared. Although the in vivo clearance of IgA purified from both Tg and non-Tg mice showed similar kinetics in B6 μMT mice (data not shown), hypoglycosylated IgA from (NZW × B6)F_1-*hbcl-2* Tg mice displayed an increased capacity to induce glomerular deposition (Fig. 8). In fact, >70% of glomeruli of (NZW × B6)F_1 non-Tg recipients injected with IgA from F_1-*hbcl-2* Tg mice showed substantial amounts of granular IgA deposits in mesangium (Fig. 8*B*), whereas IgA from F_1 non-Tg mice induced only minimal IgA deposits (Fig. 8*A*).

Discussion

Although IgAN is the most frequent form of glomerulonephritis, the cellular and molecular mechanisms involved in its pathogenesis are still largely unknown. In this study, we show that in (NZW × B6)F_1-*hbcl-2* Tg mice, defects in the regulation of B cell apoptosis, as a result of the overexpression of hBcl-2, lead to the development of IgA hypergammaglobulinemia and IgAN, in addition to a lupus-like autoimmune syndrome, and that both SLE and IgAN are dependent on the presence of $CD4^+$ T cells. The overexpression of Bcl-2 in B cells prominently enhances IgA systemic immune responses to T-dependent Ags. In addition, the levels of galactosylation and sialylation of serum IgA in (NZW × B6)F_1-*hbcl-2* Tg mice are reduced, thereby promoting their glomerular deposition. However, the absence of significant glomerular lesions in B6-*hbcl-2* Tg mice stresses the importance of the abnormal proautoimmune genetic background of NZW mice (31–34) in the pathogenesis of the disease.

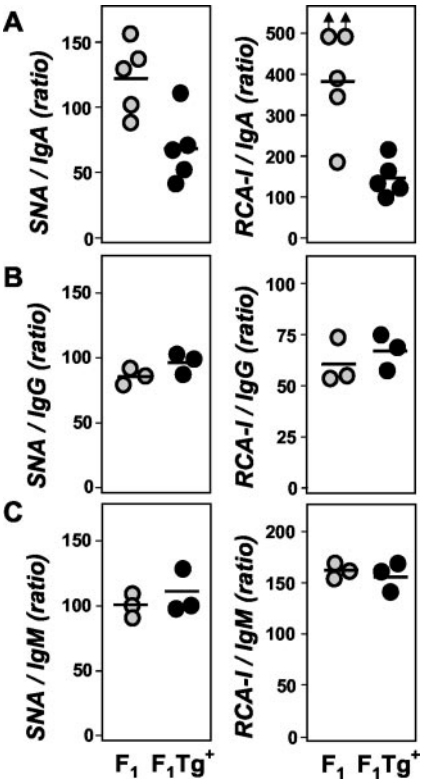

FIGURE 7. SNA and RCA-1 lectin binding by IgA (*A*), IgG (*B*), and IgM (*C*) in sera from 4- to 6-mo-old (NZW × B6)F_1-*hbcl-2* Tg (●) and (NZW × B6)F_1 non-Tg mice (○). The pattern of sialylation (*left*) and galactosylation (*right*) of IgA, IgG, and IgM purified from three to five different serum pools was assessed by measuring the binding to SNA and RCA-I, respectively. Bars represent the mean value of each examination.

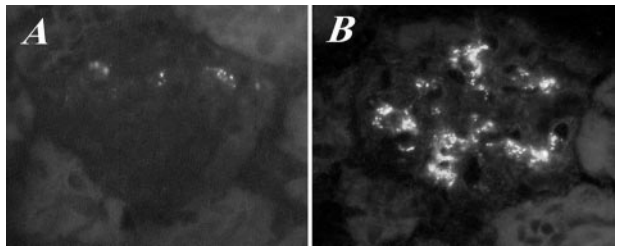

FIGURE 8. Immunofluorescence analysis of glomerular IgA deposits (×40) in 1.5-mo-old (NZW × B6)F_1 non-Tg recipients i.v. injected with 10 mg of purified IgA from (NZW × B6)F_1 non-Tg mice (*A*) or (NZW × B6)F_1-*hbcl-2* Tg mice (*B*). Representative results obtained from three mice in each group are shown.

One common immunological abnormality found in patients with IgAN is the presence of increased levels of circulating IgA (1, 2). In addition to IgG hypergammaglobulinemia, (NZW × B6)F_1-*hbcl-2* Tg, but not B6-*hbcl-2* Tg mice also exhibit high levels of IgA in their sera. Several possibilities may explain how the overexpression of Bcl-2 promotes the development of IgA hypergammaglobulinemia in (NZW × B6)F_1 mice. It has been shown recently that μMT mutant mice deficient in conventional mature B cells, because of the lack of IgM expression (22), are still able to produce significant levels of circulating IgA (42), demonstrating the existence of a unique pathway for IgA production that does not require IgM expression in B cells. Strikingly, μMT mice having defects in the regulation of B cell apoptosis due to either the overexpression of Bcl-2 or mutations in Fas display an increased number of B cell precursors that can complete their maturation program without the surface IgM expression and produce both IgG and IgA isotypes (43, 44). However, the production of IgA in μMT mice is largely independent of T cells, and these IgA-producing B cells fail to respond to exogenous Ags after immunization (42–44), in a marked contrast to the total dependency on $CD4^+$ T cells for the production of IgA in (NZW × B6)F_1-*hbcl-2* Tg mice and the development of remarkable IgA responses to T-dependent Ags in *hbcl-2* Tg mice. These results thus strongly argue against the involvement of the IgM-independent IgA induction pathway as the cause of IgA hypergammaglobulinemia in (NZW × B6)F_1-*hbcl-2* Tg mice. Additionally, because of an increase in the number of B-1 cells in human patients with IgAN (35), a possible role for this cell population in the development of the disease has been suggested. However, this possibility seems unlikely in the present experimental model, because our data clearly show the lack of expansion of peritoneal B-1 cells in (NZW × B6)F_1-*hbcl-2* Tg mice. In addition, we noted that the overexpression of hBcl-2 in B cells rather leads to a reduction in the number of MZ B cells, a B cell population that shares multiple phenotypic characteristics of B-1 cells (36). We favor the idea that conventional B-2 cells are responsible

for the increased production of IgA observed in (NZW × B6)F_1-*hbcl-2* Tg mice. It can be speculated that in the course of T-dependent immune responses, the increase in B cell survival within the germinal center, secondary to the overexpression of Bcl-2, may facilitate the isotype class switching to more downstream H chain genes such as *Cα*, simply by prolonging the duration of the B cell response. Although we failed to show any modulation of TGF-*β* mRNA in spleen between *hbcl-2* Tg and non-Tg mice, it would be of interest to explore whether any unique cytokine expression may be associated with increased IgA Ab responses in the *hbcl-2* Tg mouse model.

One intriguing observation in our study is the absence of IgG deposits in the glomeruli of (NZW × B6)F_1-*hbcl-2* Tg mice despite the elevated titers of IgG autoantibodies in their sera. These findings contrast with the demonstration of strong IgG deposits in the original *hbcl-2* Tg mice bearing a (B6 × SJL)F_2 mixed background (the presence of IgA deposits was not explored in these mice) (21). Such divergences can be partly attributed to the difference in the genetic background of mice used in the present study. Nevertheless, our present results suggest that serum IgA in (NZW × B6)F_1-*hbcl-2* Tg mice may exhibit intrinsic abnormalities that facilitate the preferential glomerular deposition. In this regard, it should be stressed that IgA, but not IgG, in these mice is hypogalactosylated and hyposialylated in comparison with IgA from non-Tg F_1 littermates. A reduced glycosylation pattern of IgA also has been observed in patients with IgAN and in HIGA mice developing an IgAN (10–13, 15). This IgA abnormality seems to play an important role in the pathogenesis of IgAN in humans, because hypoglycosylated IgA1 apparently has an increased capacity of binding to mesangial cells (12, 13). This is consistent with our present results showing that hypoglycosylated IgA from (NZW × B6)F_1-*hbcl-2* Tg mice displays an increased capacity to induce glomerular deposits, and strongly supports the notion that aberrant IgA glycosylation has an important pathogenic significance in this experimental murine model of IgAN.

The reduced pattern of oligosaccharide galactosylation and sialylation in serum IgA from (NZW × B6)F_1-*hbcl-2* Tg mice can be secondary to the presence of a particular proinflammatory cytokine environment as a consequence of the activation of the immune system observed in these autoimmune animals. An association between a Th2 hyperactivity and IgA hypoglycosylation has been reported (15, 28, 45), and the administration of IL-12, a potent Th1-inducing factor, to ddY mice increases both the galactosylation and sialylation of circulating and glomerular IgA (15). If an imbalance toward Th2 is responsible for the reduced glycosylation of serum IgA in (NZW × B6)F_1-*hbcl-2* Tg mice, we would expect reciprocal changes in serum levels of IgG1 (increase) and IgG2a (reduction), two IgG subclasses associated with Th2 and Th1 activity, respectively (46). However, an increased production of all IgG subclasses at the same extent in (NZW × B6)F_1-*hbcl-2* Tg mice argues against this possibility. Alternatively, the reduced pattern of glycosylation of IgA in (NZW × B6)F_1-*hbcl-2* Tg mice can be a direct consequence of Bcl-2 overexpression in B cells. In fact, the overexpression of Bcl-2 in Maldin-Darby canine kidney cells infected with influenza virus promotes changes in the glycosylation of viral hemagglutinin (47). It also has been shown that in Fas-deficient MRL-*lpr/lpr* mice, the proportion of IgG lacking galactose is significantly increased (48, 49). Because the Fas mutation and overexpression of Bcl-2 most likely result in increased life span of activated B cells, the expansion of some autoreactive B cell clones in an autoimmune-prone genetic background may be accompanied by a progressive decrease in galactosyltransferase activity of these aging B cells, thus favoring the appearance of undergalactosylated autoantibodies. However, we did not observe the aberrant glycosylation in IgG from (NZW × B6)F_1-*hbcl*-2 Tg mice. This may be related to the fact that Bcl-2 and Fas may regulate different survival pathways within the germinal center (50), or alternatively to the fact that the structure of oligosaccharide side chains from IgA is much more complex and heterogeneous than that from IgG (40, 48). In addition to the typical bi-antennary complex-type oligosaccharide chains attached to IgG molecules, IgA contains additional tri-antennary oligosaccharide chains (40). Galactosylation of the bi-antennary and tri-antennary chains may be catalyzed by different isoforms of galactosyltransferases (51). The selective hypogalactosylation of IgA oligosaccharides in (NZW × B6)F_1-*hbcl*-2 Tg mice may be due to a differential regulation of galactosyltransferases responsible for galactosylation in different forms of oligosaccharide chains. If so, one would expect that altered glycosylation occurring in (NZW × B6)F_1-*hbcl*-2 Tg mice should be more selective to the tri-antennary chains uniquely present in IgA. The structural and sequence analysis of the bi-antennary and tri-antennary oligosaccharide chains isolated from IgA and IgG from the *hbcl-2* Tg and non-Tg mice should help answer this question. Finally, the pattern of IgA glycosylation may also be influenced by unknown background genes present in either NZW or B6 mice. In fact, we have observed that the IgA from B6 mice is hypoglycosylated to the same extent as IgA from (NZW × B6)F_1-*hbcl*-2 Tg mice. In these hypoglycosylation conditions, the overexpression of hBcl-2 in B cells from B6 mice fails to promote an additional reduction in the levels of IgA glycosylation (R. Marquina, J. Merino, and R. Merino, manuscript in preparation). These results also suggest that the abnormal proautoimmune genetic background of NZW mice may be critical for the development of glomerular lesions in the presence of hypoglycosylated IgA.

In summary, we present evidence for a new experimental murine model of IgAN associated with SLE. In this experimental model, defects in the regulation of B cell apoptosis in genetically susceptible mice are involved in the pathogenesis of the disease. Although a relationship between inhibition of B cell death and IgAN in humans has not been reported yet, the proposed model can be of interest to study cellular and molecular mechanisms responsible for the development of this common form of glomerulonephritis.

Acknowledgments

We thank Maria Aramburu, Yolanda Trespalacios, Natalia Cobo, and Chantal Tougne for technical assistance.

References

1. Donadio, J. V., and J. P. Grande. 2002. IgA nephropathy. *N. Engl. J. Med. 347:738.*
2. Floege, J., and J. Feehally. 2000. IgA nephropathy: recent developments. *J. Am. Soc. Nephrol. 11:2395.*
3. Donadio, J. V., and J. P. Grande. 1997. Immunoglobulin A nephropathy: a clinical perspective. *J. Am. Soc. Nephrol. 8:1324.*
4. Radford, M. G., J. V. Donadio, E. G. Bergstralh, and J. P. Grande. 1997. Predicting renal outcome in IgA nephropathy. *J. Am. Soc. Nephrol. 8:199.*
5. Launay, P., B. Grossetête, M. Arcos-Fajardo, E. Gaudin, S. P. Torres, L. Beaudoin, N. Patey-Mariaud de Serre, A. Lehuen, and R. C. Monteiro. 2000. Fcα receptor (CD89) mediates the development of immunoglobulin A (IgA) nephropathy (Berger's disease): evidence for a pathogenic soluble receptor-IgA complexes in patients and CD89 transgenic mice. *J. Exp. Med. 191:1999.*
6. Casanueva, B., V. Rodriguez-Valverde, J. Merino, M. Arias, and M. Garcia-Fuentes. 1983. Increased IgA-producing cells in the blood of patients with active Henoch-Schonlein purpura. *Arthritis Rheum. 26:854.*
7. Casanueva, B., V. Rodriguez-Valverde, M. Arias, A. Vallo, M. Garcia-Fuentes, and J. Rodriguez-Soriano. 1986. Immunoglobulin-producing cells in IgA nephropathy. *Nephron 43:33.*
8. De Fijter, J. W., J. W. Eijgenraam, C. A. Braam, J. Holmgren, M. R. Daha, L. A. van Es, and A. W. van der Wall Blake. 1996. Deficient IgA1 immune response to nasal cholera toxin subunit B in primary IgA nephropathy. *Kidney Int. 50:952.*
9. Layward, L., A. C. Allen, S. J. Harper, J. M. Hattersley, and J. Feehally. 1992. Increased and prolonged production of specific polymeric IgA after systemic

immunization with tetanus toxoid in IgA nephropathy. *Clin. Exp. Immunol. 88:394*.
10. Tomana, M., K. Matousovic, B. A. Julian, J. Radl, K. Konecny, and J. Mestecky. 1997. Galactose-deficient IgA1 in sera of IgA nephropathy patients is present in complexes with IgG. *Kidney Int. 52:509*.
11. Tomana, M., J. Novak, B. A. Julian, K. Matousovic, K. Konecny, and J. Mestecky. 1999. Circulating immune complexes in IgA nephropathy consist of IgA1 with galactose-deficient hinge region and antiglycan antibodies. *J. Clin. Invest. 104:73*.
12. Hiki, Y., T. Kokubo, H. Iwase, Y. Masaki, T. Sano, A. Tanaka, K. Toma, K. Hotta, and Y. Kobayashi. 1999. Underglycosylation of IgA1 hinge plays a certain role for its glomerular deposition in IgA nephropathy. *J. Am. Soc. Nephrol. 10:760*.
13. Mestecky, J., O. H. Hashim, and M. Tomana. 1995. Alterations in the IgA carbohydrate chains influence the cellular distribution of IgA1. *Contrib. Nephrol. 111:67*.
14. Muso, E., H. Yoshida, E. Takeuchi, M. Yashiro, H. Matsushima, A. Oyama, K. Suyama, T. Kawamura, T. Kamata, S. Miyawaki, et al. 1996. Enhanced production of glomerular extracellular matrix in a new mouse strain of high serum IgA ddY mice. *Kidney Int. 50:1946*.
15. Kobayashi, I., N. Fumiaki, H. Kusano, T. Ono, S. Miyawaki, H. Yoshida, and E. Muso. 2002. Interleukin-12 alters the physicochemical characteristics of serum and glomerular IgA and modifies glycosylation in a ddY mouse strain having high IgA levels. *Nephrol. Dial. Transplant. 17:2108*.
16. Chun, H. J., and M. J. Lenardo. 2001. Autoimmune lymphoproliferative syndrome: types I, II and beyond. *Adv. Exp. Med. Biol. 490:49*.
17. Nagata, S., and T. Suda. 1995. Fas and Fas ligand: *lpr* and *gld* mutations. *Immunol. Today 16:39*.
18. Bouillet, P., D. Metcalf, D. C. Huang, D. M. Tarlinton, T. W. Kay, F. Kontgen, J. M. Adams, and A. Strasser. 1999. Proapoptotic Bcl-2 relative Bim required for certain apoptotic responses, leukocyte homeostasis, and to preclude autoimmunity. *Science 286:1735*.
19. Bouillet, P., J. F. Purton, D. I. Godfrey, L. C. Zhang, L. Coultas, H. Puthalakath, M. Pellegrini, S. Cory, J. M. Adams, and A. Strasser. 2002. BH3-only Bcl-2 family member Bim is required for apoptosis of autoreactive thymocytes. *Nature 415:922*.
20. Hildeman, D. A., Y. Zhu, T. C. Mitchell, P. Bouillet, A. Strasser, J. Kappler, and P. Marrack. 2002. Activated T cell death in vivo mediated by proapoptotic *bcl*-2 family member *bim*. *Immunity 16:759*.
21. Strasser, A., S. Whittingham, D. L. Vaux, M. L. Bath, J. M. Adams, S. Cory, and A. W. Harris. 1991. Enforced BCL2 expression in B-lymphoid cells prolongs antibody responses and elicits autoimmune disease. *Proc. Natl. Acad. Sci. USA 88:8661*.
22. Kitamura, D., J. Roes, R. Kuhn, and K. Rajewsky. 1991. A B cell-deficient mouse by targeted disruption of the membrane exon of the immunoglobulin μ chain gene. *Nature 350:423*.
23. Lopez-Hoyos, M., R. Carrio, R. Merino, L. Buelta, S. Izui, G. Nuñez, and J. Merino. 1996. Constitutive expression of Bcl-2 in B cells causes a lethal form of lupus-like autoimmune disease after induction of neonatal tolerance to $H\text{-}2^b$ alloantigens. *J. Exp. Med. 183:2523*.
24. Merino, R., L. Fossati, M. Iwamoto, S. Takahashi, R. Lemoine, N. Ibnou-Zekri, L. Pugliatti, J. Merino, and S. Izui. 1995. Effect of long-term anti-CD4 or anti-CD8 treatment on the development of *lpr* $CD4^-CD8^-$ double negative T cells and of the autoimmune syndrome in MRL-*lpr/lpr* mice. *J. Autoimmun. 8:33*.
25. Clark, J. D., G. F. Gebhart, J. C. Gonder, M. E. Keeling, and D. F. Kohn. 1997. Special report: the 1996 guide for the care and use of laboratory animals. *ILAR J. 38:41*.
26. Pihlgren, M., C. Tougne, P. Bozzotti, A. Fulurija, M. A. Duchosal, P. H. Lambert, and C. A. Siegrist. 2003. Unresponsiveness to lymphoid-mediated signals at the neonatal follicular dendritic cell precursor level contributes to delayed germinal center induction and limitations of neonatal antibody responses to T-dependent antigens. *J. Immunol. 170:2824*.
27. Reininger, L., T. Shibata, S. Schurmans, R. Merino, L. Fossati, M. Lacour, and S. Izui. 1990. Spontaneous production of anti-mouse red blood cell autoantibodies is independent of the polyclonal activation in NZB mice. *Eur. J. Immunol. 20:2405*.
28. Chintalacharuvu, S. R., and S. N. Emancipator. 1997. The glycosylation of IgA produced by murine B cells is altered by Th2 cytokines. *J. Immunol. 159:2327*.
29. Morel, L., C. Mohan, Y. Yu, B. P. Croker, N. Tian, A. Deng, and E. K. Wakeland. 1997. Functional dissection of systemic lupus erythematosus using congenic mouse strains. *J. Immunol. 158:6019*.
30. Kuroki, A., T. Moll, M. López-Hoyos, L. Fossati-Jimack, N. Ibnou-Zekri, S. Kikuchi, J. Merino, R. Merino, and S. Izui. 2004. Enforced BCL-2 expression in B lymphocytes induces rheumatoid factor and anti-DNA production, but the *Yaa* mutation promotes only anti-DNA production. *Eur. J. Immunol. 34:1077*.
31. Hsu, S. I., S. B. Ramirez, M. P. Winn, J. V. Bonventre, and W. F. Owen. 2000. Evidence for genetic factors in the development and progression of IgA nephropathy. *Kidney Int. 57:1818*.
32. Wakeland, E. K., A. E. Wandstrat, K. Liu, and L. Morel. 1999. Genetic dissection of systemic lupus erythematosus. *Curr. Opin. Immunol. 11:701*.
33. Vyse, T. J., C. G. Drake, S. J. Rozzo, E. Roper, S. Izui, and B. L. Kotzin. 1996. Genetic linkage of IgG autoantibody production in relation to lupus nephritis in New Zealand hybrid mice. *J. Clin. Invest. 98:1762*.
34. Vyse, T. J., R. K. Halterman, S. J. Rozzo, S. Izui, and B. L. Kotzin. 1999. Control of separate pathogenic autoantibody responses marks MHC gene contributions to murine lupus. *Proc. Natl. Acad. Sci. USA 96:8098*.
35. Kodama, S., M. Suzuki, M. Arita, and G. Mogi. 2001. Increase in tonsillar germinal centre B-1 cell numbers in IgA nephropathy (IgAN) patients and reduced susceptibility to Fas-mediated apoptosis. *Clin. Exp. Immunol. 123:301*.
36. Berland, R., and H. H. Wortis. 2002. Origins and functions of B-1 cells with notes on the role of CD5. *Annu. Rev. Immunol. 20:253*.
37. Brunner, C., D. Marinkovic, J. Klein, T. Samardzic, L. Nitschke, and T. Wirth. 2003. B cell-specific transgenic expression of Bcl2 rescues early B lymphopoiesis but not B cell responses in BOB.1/OBF.1-deficient mice. *J. Exp. Med. 197:1205*.
38. Letterio, J. J., and A. B. Roberts. 1998. Regulation of immune responses by TGF-β. *Annu. Rev. Immunol. 16:137*.
39. Cazac, B. B., and J. Roes. 2000. TGF-β receptor controls B cell responsiveness and induction of IgA in vivo. *Immunity 13:443*.
40. Lipniunas, P., G. Gronberg, H. Krotkiewski, A. S. Angel, and B. Nilsson. 1993. Investigation of the structural heterogeneity in the carbohydrate portion of a mouse monoclonal immunoglobulin A antibody. *Arch. Biochem. Biophys. 300:335*.
41. Roccatello D., G. Picciotto, M. Torchio, R. Ropolo, M. Ferro, R. Franceschini, G. Quattrocchio, G. Cacace, R. Coppo, and L. M. Sena. 1993. Removal systems of immunoglobulin A and immunoglobulin A containing complexes in IgA nephropathy and cirrhosis patients: the role of asialoglycoprotein receptor. *Lab. Invest. 69:714*.
42. Macpherson, A. J. S., A. Lamarre, K. Mccoy, G. R. Arriman, B. Odermatt, G. Dougan, H. Hengartner, and R. M. Zinkernagel. 2001. IgA production without μ or δ chain expression in developing B cells. *Nat. Immunol. 2:625*.
43. Tarlinton, D. M., L. M. Corcoran, and A. Strasser. 1997. Continued differentiation during B lymphopoiesis requires signals in addition to cell survival. *Int. Immunol. 9:1481*.
44. Melamed, D., E. Miri, N. Leider, and D. Namazee. 2000. Unexpected autoantibody production in membrane Ig-μ-deficient/*lpr* mice. *J. Immunol. 165:4353*.
45. Chintalacharuvu, S. R., N. U. Nagy, N. Sigmund, J. G. Nedrud, M. E. Lamm, and S. N. Emancipator. 2001. T cell cytokines determine the severity of experimental IgA nephropathy by regulating IgA glycosylation. *Clin. Exp. Immunol. 126:326*.
46. DeKruyff, R. H., L. V. Rizzo, and D. T. Umetsu. 1993. Induction of immunoglobulin synthesis by $CD4^+$ T cell clones. *Semin. Immunol. 5:421*.
47. Olsen, C. W., J. C. Kehren, N. R. Dybdahl-Sissoko, and V. S. Hinshaw. 1996. *bcl-2* alters influenza virus yield, spread and hemagglutinin glycosylation. *J. Virol. 70:663*.
48. Mizuochi, T., J. Hamako, M. Nose, and K. Titani. 1990. Structural changes in the oligosaccharide chains of IgG in autoimmune MRL/Mp-*lpr/lpr* mice. *J. Immunol. 145:1794*.
49. Bond, A., A. Cooke, and F. C. Hay. 1990. Glycosylation of IgG, immune complexes and IgG subclasses in the MRL-*lpr/lpr* mouse model of rheumatoid arthritis. *Eur. J. Immunol. 20:2229*.
50. Strasser, A., A. W. Harris, D. C. Huang, P. H. Krammer, and S. Cory. 1995. Bcl-2 and Fas/APO-1 regulate distinct pathways to lymphocyte apoptosis. *EMBO J. 14:6136*.
51. Amado, M., R. Almeida, T. Schwientek, and H. Clausen. 1999. Identification and characterization of large galactosyltransferase gene families: galactosyltransferases for all functions. *Biochim. Biophys. Acta 1473:35*.